Res Nondestr Eval (2000) 12:31–42

DOI: 10.1007/s001640000003

Nonlinear Elastic Wave Spectroscopy (NEWS) Techniques to Discern Material Damage, Part II: Single-Mode Nonlinear Resonance Acoustic Spectroscopy

K. E.-A. Van Den Abeele,[1] J. Carmeliet,[1] J. A. Ten Cate,[2] P. A. Johnson[2]

[1]Department of Building Physics, Catholic University Leuven, Belgium
[2]Los Alamos National Laboratory, Los Alamos, NM 875454, USA

Abstract. The presence of mesoscopic features and damage in quasi-brittle materials causes significant second-order and nonlinear effects on the acoustic wave propagation characteristics. In order to quantify the influence of such micro-inhomogeneities, a new and promising tool for nondestructive material testing has been developed and applied in the field of damage detection. The technique focuses on the acoustic nonlinear (i.e., amplitude-dependent) response of one of the material's resonance modes when driven at relatively small wave amplitudes. The method is termed single-mode nonlinear resonance acoustic spectroscopy (SIMONRAS). The behavior of damaged materials is manifested by amplitude dependent resonance frequency shifts, harmonic generation, and nonlinear attenuation. We illustrate the method by experiments on artificial slate tiles used in roofing construction. The sensitivity of this method to discern material damage is far greater than that of linear acoustic methods.

1. Introduction

The elastic behavior of brittle materials such as brick, slate, concrete, rock, sand, and soil is manifest by strong nonlinearity, hysteresis in stress–strain relation, and discrete memory. Primarily, it is the materials' compliance, represented by the mesoscopic linkages (order 10^{-6}–10^{-9} m) between the rigid components, that gives these materials their unusual elastic properties. Materials with nonlinear *mesoscopic elasticity* stand in contrast to liquids and crystalline solids whose elasticity is due to contributions of atomic level forces, i.e., materials with *atomic elasticity*. Atomic elastic materials are well described by the traditional theory of elasticity [1, 2]; however, mesoscopic elastic materials are not. For low strain levels, mesoscopic materials are well described by the Preisach-Mayergoyz (P-M) model of nonlinear elasticity, as developed in the mesoscopic model by McCall and Guyer [3, 4]. A sequence of experiments on numerous intact and microcracked materials illustrates the evidence of nonlinear mesoscopic elastic behavior and yields the significant conclusion that *damaged atomic elastic materials behave as mesoscopic elastic materials* [5, 6]. Qualitatively, the amount

of nonlinearity is highly correlated to the damage/microcracked state of the material [7].

Recently a couple of promising and powerful nondestructive evaluation (NDE) tools for damage interrogation in materials have been developed. The methods basically study the amplitude-dependent frequency response in dynamic wave experiments, and are termed nonlinear elastic wave spectroscopy (NEWS) techniques. One method is nonlinear wave modulation spectroscopy (NWMS) and is described in Part I [8, 9]. In short, NWMS is based on the monitoring of nonlinear frequency mixing in the material. The manifestations of the nonlinear response appear as wave distortion and accompanying wave harmonics, and in sum and difference frequency generation (sidebands). The approach has proved to be time efficient and effective in discerning damage to materials. The second method is called nonlinear resonant ultrasound spectroscopy (NRUS): the study of the nonlinear response of a single, or a group of, resonant modes of the material [5, 10, 11]. Granular and microcracked materials always show nonlinear softening of the elastic modulus with increasing drive levels in dynamic resonance experiments, even at strains as low as 10^{-8}. As a result, the resonance frequency shifts, harmonics are generated, and amplitude-dependent damping characteristics are observed. In undamaged materials, these phenomena are very weak. In damaged materials, they are remarkably large.

In this paper we focus on the NRUS technique and its application to damage detection. In a previous publication, we constructed a diagnostic method which is used to quantify the acoustic nonlinearity of homogenous and isotropic samples in laboratory benchtop resonance experiments [11]. The analysis of the experimental data is supported by a phenomenological model based on the P-M implementation of hysteresis. In general, six material parameters—two linear and four nonlinear—can be extracted from the data. These six parameters completely define the material state of the sample (depending on confining pressure, saturation, damage, etc.) and may be found from a simple set of nonlinear experiments: (1) measure the relative frequency shift as a function of measured acceleration, (2) measure the amplitude dependence of the measured second and third harmonic levels, and (3) measure the relaxation of the linear modulus after high excitation.

The characterization procedure is applied to damage detection in thin slate beams. We investigate the first-order bending mode, which has a resonance frequency well below 500 Hz (acoustic resonance). Linear (wave speed and wave dissipation) and nonlinear parameters were measured for progressive fatigue, induced by cyclic mechanical loading. We will show that the sensitivity of nonlinear methods to the detection of damage features (cracks, flaws, etc.) is far greater than that of linear acoustical methods.

2. Experiment and Configuration

The experimental apparatus used to obtain the results discussed in this paper is shown in Fig. 1. A similar configuration for the study of cylindrical cores is described and used by TenCate and Shankland [10] and by Van Den Abeele and TenCate [11]. The samples are thin, rectangular beams of artificial slate used in roofing construction. The major component in their composition is Portland cement. Mineral additives and synthetic

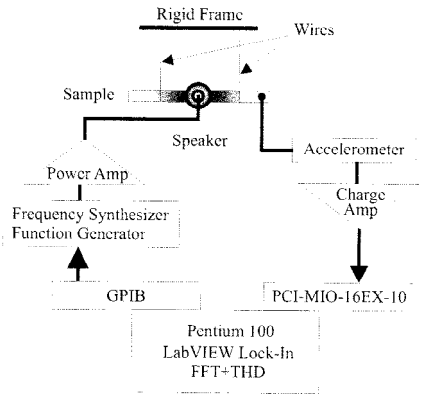

Fig. 1. Experimental setup for SIMONRAS experiments.

organic fibers are added for strength enhancement. The open porosity is about 26%. The nominal dimensions of the beams used in the present study are 200 mm × 20 mm ×4 mm.

The beams are excited at their lowest-order bending resonance mode by a low-frequency, low-distortion speaker. The displacement distribution corresponding to this resonance has two nodal positions (at $0.224 \times L$ from the edges, with L the length of the beam) from which the samples are supported by thin nylon wires. The strain concentration is located in the middle of the beam. The first-order resonance frequency is typically of order 300 Hz, and the linear attenuation, measured from the resonance width and expressed as a modal damping ratio ξ, equals 0.005 (i.e., a quality factor Q of 100, since $Q = \frac{1}{2}\xi$) [12]. The speaker is positioned at 2 cm from the middle, parallel to the beam surface. It is driven in discrete frequency steps by a function generator through a high-power amplifier. The coupling medium between specimen and speaker is air (noncontact excitation). A B&K 4375 accelerometer attached to one end of the beam measures the sample's out-of-plane response. The signal from the accelerometer is preamplified, fed into a 16-bit A/D convertor, and analyzed using LabVIEW. A lock-in virtual instrument is used to measure the fundamental frequency level. The harmonic content is analyzed using LabVIEW's "Harmonic Analyzer"-vi. The apparatus is capable of measuring accelerations down to 10^{-2} m/s^2, which typically corresponds to inferred strains of 10^{-9} for rectangular beam samples of 200 mm in length and 4 mm in thickness. In order to monitor resonant peak shift and harmonic generation, 4 to 10 resonance sweeps are made at successively increasing drive voltages over the same frequency interval. With Q ("inverse attenuation," $\frac{1}{2}\xi$) being 100, a single sweep is typically 1 min in duration, depending on the frequency step size. Sweep rates, step sizes, and data storage are all PC controlled.

In a sample that is intact (atomic), the resonance curves scale linearly with the applied voltage. The resonance frequency and the attenuation are amplitude independent, and there is no evidence of harmonic generation. In a sample that is damaged (or nonlinear mesoscopic to begin with), one observes an amplitude-dependent resonance frequency

shift (a softening of the modulus, in general), harmonics are created by the nonlinearity of the medium, and the attenuation increases significantly with drive voltage. Based on the P-M model, the relationship between the drive amplitudes and the various nonlinear phenomena provides clues to the type of nonlinearity of the material [11, 13]. The presence of such nonlinear effects indicates microcracking and damage [7].

Figure 2 illustrates the experimental results for a slate sample before and after damage impact. The resonance curves for the intact sample do not clearly show signs of softening. However, analysis of the resonance maxima, i.e., plotting the relative resonance frequency shift, $(f_0 - f)/f_0$ (with f_0 the linear resonance frequency and the f the resonance frequency at increasing drive voltage), versus the measured peak acceleration, reveals a slight linear decrease of the resonance frequency with increasing amplitude. The measured harmonics, obtained at peak resonance, are all at least 60 dB below the fundamental. The attenuation factor ξ is barely increasing with amplitude [$(\xi - \xi_0)/\xi_0$ is plotted, where ξ_0 is the modal damping ratio at low strain and ξ is the attenuation at increasing drive voltage]. For the damaged sample, the softening becomes significantly more apparent. A similar analysis of the resonance frequency shows that the nonlinear effect is raised by two orders of magnitude due to the induced microdamage. The amplitude dependence is still linear. Also, with the greater frequency shift, the harmonic spectrum changes dramatically. The third harmonic becomes dominant, and its dependence on the fundamental acceleration amplitude is quadratic. It is remarkable that the second harmonic does not show nearly a similar increase. Finally, we observe a significant increase in nonlinearity of the damping. The attenuation depends linearly on the measured resonance amplitude. (For a method to invert the attenuation in the case of a skewed resonance peak, we refer the reader to the work of Smith and TenCate [14].)

3. Phenomenological Model

The linear resonance frequency shift, the quadratic amplitude dependence of the third harmonic, and the linear increase of the attenuation with increasing drive level are typical observations of mesoscopic hysteretic materials. From various static and dynamic experiments we do know that microcracked materials cannot be described by classical theory. When cracked, intact materials become highly nonlinear, and/or exhibit hysteresis and discrete memory in their stress–strain relation [6]. As discussed in Part I, the theoretical description of nonlinear mesoscopic elastic materials contains terms that describe classical nonlinearity, as well as hysteresis, and discrete memory [3, 4, 13, 15–18]. In order to describe the typical observations illustrated later, in Fig. 3, it suffices to account only for hysteretic effects (i.e., the effect of classical anharmonicity of the energy density is negligible). In this case, the constitutive relation between the stress σ and the strain ε can be expressed as follows:

$$\sigma = \int K(\varepsilon, \dot{\varepsilon})\, d\varepsilon, \tag{1a}$$

with K the nonlinear hysteretic modulus (neglecting the classical perturbation terms), given by

$$K(\varepsilon, \dot{\varepsilon}) = K_0\{1 - \alpha[\Delta\varepsilon + \varepsilon(t)\ \mathrm{sign}(\dot{\varepsilon})] + \cdots\}. \tag{1b}$$

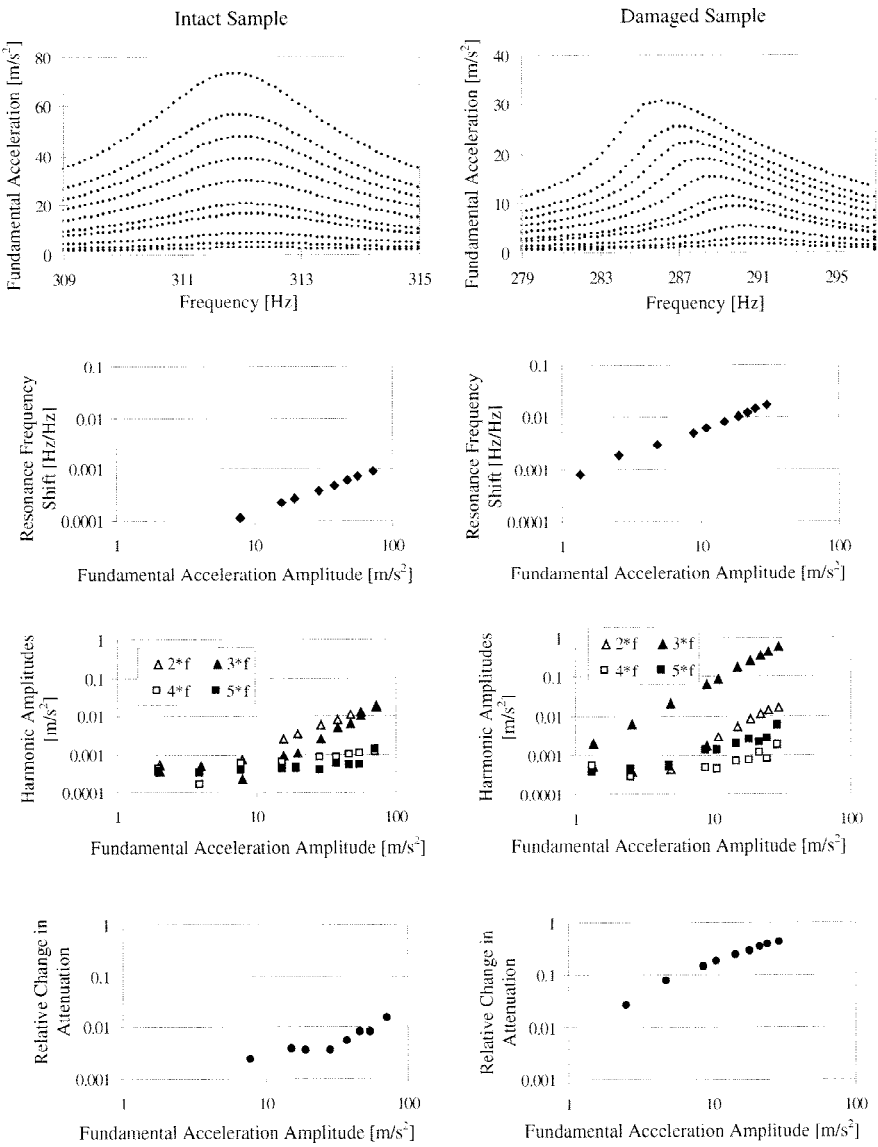

Fig. 2. Single–mode nonlinear resonance acoustic spectroscopy of the first bending mode of an intact (left) and a microdamaged slate beam (right): *top row*, measured resonance curves at 10 different drive levels; *second row*, relative resonant frequency shift $(f_0 - f)/f_0$ as a function of the peak acceleration amplitude measured at the different drive levels; *third row*, harmonic content at peak acceleration; *bottom row*, relative change of the measured attenuation $(\xi - \xi_0)/\xi_0$ as a function of peak accelerations.

Here, K_0 is the linear modulus, $\Delta\varepsilon$ is the local strain amplitude over the previous period [$\Delta\varepsilon = (\varepsilon_{\mathrm{Max}} - \varepsilon_{\mathrm{Min}})/2$ for a simple continuous sine excitation], $\dot{\varepsilon} = d\varepsilon/dt$ the strain rate, $\mathrm{sign}(\dot{\varepsilon}) = 1$ if $\dot{\varepsilon} > 0$ and $\mathrm{sign}(\dot{\varepsilon}) = -1$ if $\dot{\varepsilon} < 0$ [13, 18]. The parameter α is a measure of the material hysteresis. A hysteretic nonlinear stress–strain relation as described in first-order approximation by Eq. (1) is capable of explaining the above-described dependencies. Indeed, substituting Eq. (1a) into the wave equation and calculating the nonlinear contribution to the solution, we find (1) a linear decrease of the resonance frequency for increasing strain levels,

$$\frac{f_0 - f}{f_0} = C_1\,\Delta\varepsilon; \tag{2}$$

(2) a quadratic amplitude dependence of the third harmonic,

$$\Delta\varepsilon_3 = C_2\,\Delta\varepsilon^2; \tag{3}$$

and (3) a linear increase of the modal damping ratio (decrease of the quality factor Q),

$$\frac{\xi - \xi_0}{\xi_0} = C_3\,\Delta\varepsilon. \tag{4}$$

The coefficients C_i in all three relationships are proportional to the hysteresis parameter α. Thus, any increase of these coefficients reflects an increase of the nonlinear hysteretic behavior of the material. Finally, it can also be shown that hysteresis does not affect the level of the even harmonics [18].

It is important to note that these results are essentially different from these for a classical nonlinear oscillator, such as the Duffing-type oscillator [19]. A classical treatment of nonlinear oscillations, using a power-law expansion of the constitutive equation, always predicts a quadratic decrease of the resonance frequency with increasing drive voltage, together with a cubic amplitude dependence of the third harmonic amplitude. Furthermore, their will be no nonlinear energy dissipation in a classical system. The experimental data shown in Fig. 2 clearly argue that hysteresis is fundamental in the description of nonlinear phenomena in quasi-brittle materials.

4. Results

In a preliminary experiment we induced progressive damage in a beam of slate by consecutive hammer impacts (10 sessions) concentrated in a region around the middle of the beam (where the strain in the first bending mode is known to be largest). After each impact, a set of 10 resonance curves was measured at increasing drive voltage. Figure 3 illustrates the analyzed data for the amplitude-dependent frequency shift and third harmonic generation in the impact experiment. The frequency shift shows a linear dependence on the fundamental acceleration amplitude for all cases. The third harmonic invariably displayed a quadratic amplitude dependence. With increasing number of impacts, we observed significant increase of the proportionality factors, and consequently, of the hysteretic strength parameter α. The relative increase before and after the impact

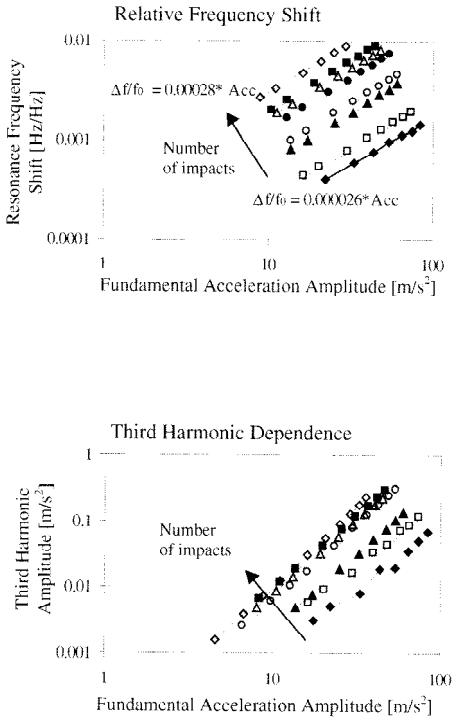

Fig. 3. SIMONRAS results for the assessment of progressive damage in the hammer impact experiment: *top*, logarithmic representation of the relative resonance frequency shift as a function of the resonance peak acceleration at different stages in the impact experiment; *bottom*, idem for the amplitude dependence of the third harmonic.

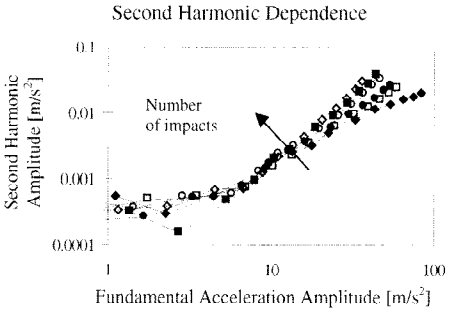

Fig. 4. Logarithmic representation for the amplitude dependence of the second harmonic at various stages in the hammer impact experiment.

sessions equals 10. A similar increase was noted for the attenuation (not shown). However, as illustrated by Fig. 4, the second harmonic did not show a significant increase. This is no surprise: hysteresis has little effect on the even harmonics, which are typically the results of anharmonicity of the elastic energy (as treated in classical nonlinear theory).

Despite the increase of the nonlinearity by a factor of 10, there was no evidence of macrocracking from the surface. We believe that the increase is due entirely to the local increase of the microcrack density in the middle of the beam.

Nonlinearity is essentially linked to the stress–strain relation. Nonlinear effects will preferably emerge at locations where stress and strain are larger. During the impact experiment, all impacts were concentrated around the middle of the beam, exactly where the strain for the first bending mode is largest. As a test we also performed impacts on the edges of the beam. There was no significant increase of the nonlinearity for these measurements.

In addition to the nonlinear measurements, analysis of the lowest-amplitude resonance curves after each impact provided two linear material parameters: resonance frequency and linear attenuation. The relative reduction of the linear (low-amplitude) resonance frequency before and after the impact sessions was only 5%. The linear attenuation (modal damping ratio) increased by 70%. Linear damping is thus significantly more sensitive to microcracking than the resonance frequency (or Young's modulus), but the relative change (1000%) in the nonlinearity parameter is far superior. It is obvious that measuring the nonlinear properties of a material will be more efficient in the detection of microcracking and can therefore be used earlier in the damage process.

The second experiment aimed at damage assessment by nonlinear resonance during controlled quasi-static fatigue loading. Three slate beams were subjected to mechanical aging by means of three-point-bending (two supports and one force cel acting in the middle of the beam). The applied load was cycled between 0 and 28 N, which is high enough to induce permanent fatigue damage after several hundreds of cycles. Each cycle took about 12 s. A fourth identical beam served as reference and was cycled between 0 and 15 N.

The typical response in force–displacement space to continuous cycle loading is shown in Fig. 5. One can distinguish three regions: (1) the elastic regime where damage by microcracking is minimal; (2) the plastic regime, where progressive damage occurs in the form of microcracking, with continuously increasing permanent deformation as a result; (3) the terminal regime, where microcracks coalesce to form a macrocrack, and lead eventually to complete failure of the material. After each cycle during the test, the computer-controlled apparatus calculates the apparent instantaneous modulus, E, from the quasi-static force–displacement curves. This value is then compared to the initial value, E_0, and used to define a damage index D, such that $D = 1 - E/E_0$. In the elastic regime, there is almost no reduction of the Young's modulus: $D \simeq 0.0$. In the plastic regime, the modulus is continuously softening: $0.0 < D < 0.5$. Finally, the modulus decreases quickly and drastically in the terminal regime: $D > 0.5$.

Single-mode nonlinear resonance acoustic spectroscopy (SIMONRAS) was used to measure the linear and nonlinear parameters of the beams at regular instances in the degradation process. The analyzed results for one of the beams are illustrated in Fig. 6. Each time, 10 resonance curves were taken at increasing drive levels. The measurements were taken in the elastic, the plastic, and the terminal regimes. A significant increase of

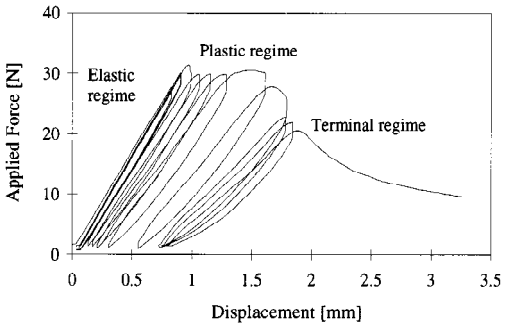

Fig. 5. Typical force–displacement evolution during cyclic fatigue loading on a slate beam in three-point bending.

the resonance frequency shift and the third harmonic levels can be observed in going from the elastic to the plastic regime (Figs. 6a and b). The fatigue damage is completely controlled by microcracks. No macrocracks are visible at this stage. In the terminal stage, a macrocrack develops at the surface. Note that the linear resonance frequency shift and quadratic power law for the third harmonic are verified through all stages of the fatigue loading experiment. Near failure, the nonlinearity coefficient deduced from the resonance frequency shift increases by a factor of 830 compared to the value in the elastic regime. A similar increase is noted in the dependence of the third harmonic. The second harmonic levels do not change significantly in the plastic regime. Only when the macrocrack appears does its proportionality to the square of the fundamental suddenly increase by a factor of order 100 (Fig. 6c).

Just as in the case of the hammer impact experiment, we followed the evolution of the linear material parameters as a function of the fatigue damage. Figure 7a illustrates the evolution of the linear resonance frequency of the first bending mode and the linear attenuation, relative to their initial values, in terms of the damage parameter D for all four beams. Note, however, that D is defined in terms of the *local* Young's modulus measured in the middle of the beam. Indeed, three-point bending specifically induces damage in the middle of the sample. In reality, the true Young's modulus is larger. Therefore, the damage factor introduced above must be considered as an indicator of local damage; the global damage factor D is smaller. Anyway, Fig. 7a clearly illustrates that measures of linear damping are more sensitive to damage than the changes in the linear resonance frequency. At the macrocrack stage, the attenuation increased by a factor of 3.2, while the linear resonance frequency is reduced only by 25%.

In addition to the linear parameters, we plotted the relative evolution of the nonlinear frequency shift parameter in Fig. 7b (note the change to logarithmic scale for the Y axis compared to Fig 7a). Again it is obvious that the investigation of the nonlinear material properties is superior to assess micro- and macrodamage. The sensitivity and detection limit improve significantly by choosing a nonlinear technique over a linear method. This implies that nonlinear parameters can be used to detect damage at a much earlier stage of degradation.

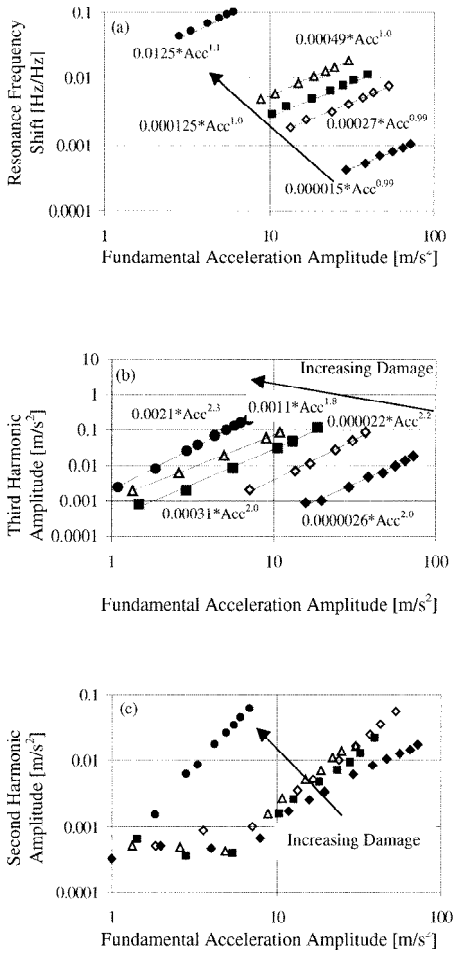

Fig. 6. Cyclic fatigue loading experiment: (a) relative resonance frequency shift as function of the measured peak acceleration amplitude at different stages in the fatigue process; (b) idem for the amplitude dependence of the third harmonic; (c) idem for the second harmonic.

5. Conclusions

Based on the experimental SIMONRAS results, quasi-brittle materials such as slate (and many other cementitious materials) exhibit nonclassical, amplitude-dependent behavior. Their nonlinearity is manifested by a linear dependence of the resonance frequency on the measured resonance peak acceleration. Their attenuation is also linearly increasing with amplitude and the third harmonic shows a quadratic dependence. These three

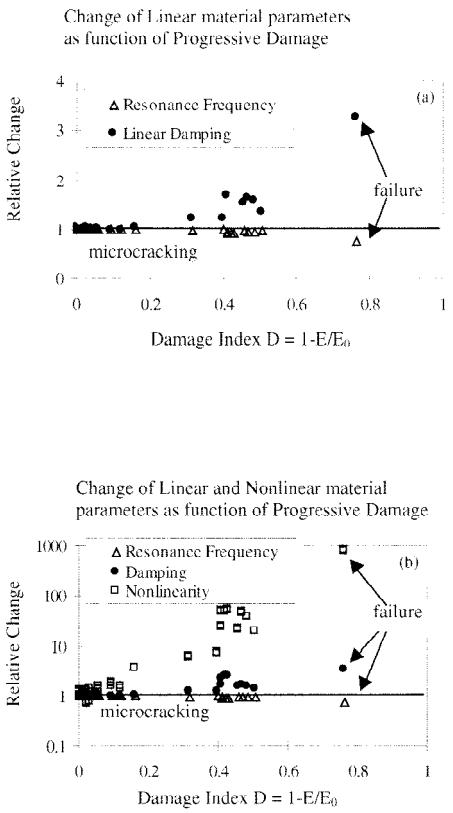

Fig. 7. Cyclic fatigue loading experiment: (a) variation of the linear material parameters (resonance frequency and attenuation) with respect to their initial values as function of the damage index D; (b) idem, with the addition of the variation of the nonlinear parameter (in logarithmic scale).

observations cannot be explained by classical nonlinear theory. Nonlinear models do require the incorporation of hysteresis in the constitutive equations. In fact, the hysteretic nonlinearity in these materials completely dominates the classical atomic nonlinearity. Micromodeling of the complex nonlinear hysteretic compliance of cracks and flaws is essential in simulating the macroscopic features observed in the nonlinear dynamics of quasi-brittle materials.

The nonlinear mesocopic nature of quasi-brittle materials becomes even more apparent when damaged. Significant increase of the nonlinearity has been observed after hammer impact, and during mechanical cyclic fatigue loading. The progressive damage/fatigue experiments discussed in this paper clearly illustrate that the sensitivity of nonlinear methods to the detection of damage features is far greater than any linear acoustical method. Therefore, acoustic diagnostic methods that focus on nonlinear phe-

nomena such as wave distortion by creation of harmonics, nonlinear attenuation, and amplitude-dependent resonance frequency shift have a strong potential in damage detection.

The nonlinear resonance technique is a relatively fast and efficient technique to assess global damage in a material. It can be applied to any type of geometry. Other nonlinear methods, such as nonlinear wave modulation spectroscopy (NWMS) [8], can be applied as a complementary technique to investigate more localized damage.

In the near future, we expect that the methodology of nonlinear elastic wave spectroscopy (NEWS) techniques will be developed and applied for various materials testing procedures. Their impact on the economy and safety can be enormous. Nonlinear methods may be implemented in applications as diverse as general production quality control (fail/pass tests), monitoring fatigue damage in composites, buildings, bridges, investigating high-temperature resistance of ceramics and concrete (fire damage), examining welding bonds in gas and oil pipelines, inspecting aircraft and spacecraft, etc.

Acknowledgments. This research has been financed by a research grant of the Flemish Institute for the promotion of scientific and technological research in the industry (IWT, Brussels, Belgium); by the Research Council of the Catholic University Leuven, Belgium; by the Office of Basic Energy Research, Engineering and Geoscience (contract W-7405-ENG-36); and by a University Collaborative Research Program of The Institute of Geophysics and Planetary Physics at Los Alamos National Laboratory, NM, USA.

References

1. L. D. Landau and E. M. Lifshitz. *Theory of Elasticity*. Pergamon, Tarrytown, NY (1959).
2. M. F. Hamilton. In *Nonlinear Wave Propagation in Mechanics*, **AMD-77**. The American Society of Mechanical Engineers, New York (1986).
3. K. R. McCall and R. A. Guyer. *J. Geophys. Res*. **99**:23887 (1994).
4. K. R. McCall and R. A. Guyer. *Nonlinear Proc. Geophys*. **3**:89 (1996).
5. P. A. Johnson, B. Zinszner, and P. N. J. Rasolofosaon. *J. Geophys. Res*. 11553 (1996).
6. P. A. Johnson and R. A. Guyer. *Phys. Today*, in press (1999).
7. See references [1–12] in Part I, this issue (1999).
8. K. Van Den Abeele, P. A. Johnson, and A. M. Sutin. This issue (1999).
9. A. M. Sutin and D. M. Donskoy. *Proc. Int. Soc. Opt. Eng*. **3397**:226 (1998).
10. J. A. TenCate and T. J. Shankland. *Geophys. Res. Lett*. **23**(21):3019 (1996).
11. K. Van Den Abeele and J. A. TenCate. Submitted for publication (1999).
12. E. E. Ungar and E. M. Kerwin. *J. Acoust. Soc. Am*. **34**(7):954 (1962).
13. R. A. Guyer, K. R. McCall, and D. Van Den Abeele. *Geophys. Res. Lett*. **25**:1585 (1998).
14. D. E. Smith and J. A. TenCate. *Geophys. Res. Lett*., in review (1999).
15. V. E. Gusev, W. Lauriks, and J. Thoen. *J. Acoust. Soc. Am*. **103**(5):3216 (1998).
16. R. A. Guyer, K. R. McCall, and G. N. Boitnott. *Phys. Rev. Lett*. **74**:3491 (1994).
17. V. E. Nazarov, L. A. Ostrovsky, I. A. Soustova, and A. M. Sutin. *Phys. Earth Planet. Interiors* **50**:65 (1988).
18. K. Van Den Abeele, P. A. Johnson, R. A. Guyer, and K. R. McCall. *J. Acoust. Soc. Am*. **101**(4):1885 (1997).
19. J. J. Stoker. *Nonlinear Vibrations in Mechanical and Electrical Systems*. Interscience, New York (1950).